Defense Technical Information Center Compilation Part Notice

ADP013758

TITLE: Eye-Ball Rebuilding Using Splines with a View to Refractive Surgery Simulation

DISTRIBUTION: Approved for public release, distribution unlimited

This paper is part of the following report:

TITLE: Algorithms For Approximation IV. Proceedings of the 2001 International Symposium

To order the complete compilation report, use: ADA412833

The component part is provided here to allow users access to individually authored sections of proceedings, annals, symposia, etc. However, the component should be considered within the context of the overall compilation report and not as a stand-alone technical report.

The following component part numbers comprise the compilation report:
ADP013708 thru ADP013761

Eye-ball rebuilding using splines with a view to refractive surgery simulation

Mathieu Lamard

Laboratoire de Traitement de l'Information Médicale, Ecole Nationale Supérieure des Télécommunications de Bretagne, F-29609 Brest Cedex, France.
Mathieu.Lamard@enst-bretagne.fr

Béatrice Cochener

CHU de Brest Ophtalmologie, 5 avenue Foch 29609 Brest Cedex, France.
Beatrice.Cochener-Lamard@chu-brest.fr

Alain Le Méhauté

Département de Mathématiques, UMR 6629, CNRS, Université de Nantes, BP 92208, F-44072 Nantes, Cedex 3, France
Alain.Le-Mehaute@math.univ-nantes.fr

Abstract

In this paper we present a use of splines in the biomedical field.

1 Introduction

In the surgical field of ophthalmology, refractive surgery has experiencied an important expansion for about fifteen years. It allows the surgeons to correct different refractive errors (myopia, hyperopia, astigmatism) aiming to decrease or minimize the use of optical equipments such as glasses and lenses. Many surgical techniques are today available for experts; with specific indications for each of them. Development of these methods commonly takes time and requires many research studies on animals before any clinical approach. In overall, abacus are established for all procedures. They provide to the surgeon some rules for the achievement of the surgery. These nomograms are usually based on statistical analysis of first wide series of operated patients. However, up to now, no technique is able to take into account individual variability of eyes (morphology, physiology).

The purpose of the present article is to consider this parameter in building a 3 dimensional numerical model of the eye and then applying to it various simulations of surgical techniques in order to measure their effects.

2 Eye and vision

2.1 The eye anatomy

Schematically the eye-ball has quite a spherical shape with a vertical diameter (approximately 23 mm) and an antero-posterior of 2 mm longer (axial length). Its average volume is 6.5 cm^3 for a weight of 7 grams.

2.2 Refractive errors

When parallels rays reach a normal eye, they are refracted and converge without accommodation on the retina (called emmetropia). Errors of refraction come from a disparity between the refractive capacity of the anterior segment of the eye and the length of the eye; the light rays are no longer focus on the retina. This is called ametropia, and is mainly of three types; myopia, hyperopia, astigmatism.

3 Correction of ametropia

3.1 Optical equipment

Glasses or lenses represent the traditional method. Glasses are safe and reversible for correction of most refractive errors but they can be responsible for visual field reduction and prismatic aberrations. They can also be a source of discomfort and cosmetic impairment for the wearer. Contact lenses have solved most of the problems associated with glasses, but require very strict hygiene to avoid severe complications. Refractive surgeries can bring an answer to these various problems.

3.2 Refractive surgery

Many techniques are available today in refractive surgeries. Most of them plan to reshape the cornea using of an excimer laser (193 nm). This laser (emitting in far UV) is used in two distinct surgeries;
— The Photo Refractive Keratomileusis (PRK)
— Laser Assisted In Situ Keratomileusis (LASIK).
The PRK technique removes cornea tissue on its surface in breaking molecular bindings. The depth and size of the ablation is determined as a function of the attempted correction. In LASIK the ablation is performed after the cut of a thin cornea flap (160 μm). This flap is replaced on the area of stromal ablation. In general PRK is used for correction of low ametropia and LASIK for low and medium corrections. For height corrections other concepts have been developed (additive surgery).

4 Data acquisition

In order to reconstruct the eyeball in 3D, data from the eye under consideration are needed. Numerous modalities allow us to obtain information about the eye anatomy.

4.1 Ultrasound

Ultrasound scan uses ultrasound waves for investigating human tissues in vivo. Nowadays in ophthalmology it is a routine exam for the posterior segment of the eye, especially for the research of foreign intra-ocular body. Reasons for this intense use are multiple,

including non invasive procedure, speed and low cost. But problems remain, which define the current limits ultrasound. Multiple phenomena of reflection (between two internal interfaces, or between an interface and a transducer itself) create false echos. Inaccuracies quickly increase with the deepening of the investigation because of all sources of "background noise", such as diffraction, diffusion and refraction. Advantages of ultrasound allowed us to use it without constraint to obtain maximum image quality. Our first work was to set up an images acquisition protocol of quality. The protocol privileged the underwater method to obtain a good acoustic coupling between the probe and the eye. The patient is lying on his back, he is wearing on his face a submarine mask without pane. This mask is filled with physiological serum. The probe, equipped with a lighting target, is plunged into the liquid. The patient fixes the target, in such conditions the provided images are along the optical axis. The operator turns this probe manually and regularly around the optical axis, and obtains a volume of data. A computer equipped with an image acquisition board can save all images on an hard disk. The images resolution is dependent on the probe and on the frequency of the ultrasound used.

4.2 MRI

The MRI, which tries to localize hydrogen pits by measuring their magnetization, realizes a real grey scale cartography of the proton concentration of the various examined structures [1]. The resultant data volume has a dependent acquisition time resolution, which currently represents one of the main important limitations of this technique. Besides the big quality of images obtained, the MRI has probably no harmful effect because it does not use ionisants beams.

4.3 Computerized corneal topography

The anterior surface of the cornea is one fundamental element of the refraction. Any modification or abnormality of this surface modifies the visual acuity. So the knowledge of this shape is extremely important. In a traditional way the Javal's keratometer is used to know punctually the refractive power of the cornea. In the last few years ophthalmologists have become used to another system, computerized corneal topography [2]. This technique, based on the reflection and the analysis of the Placido's discs deformation, allows us to obtain numerous data on the topology of the cornea. The curvature of the cornea is represented on a colored map.

4.4 Visible Human images

The images of the Visible Human project (the photographic modality) have great space resolution. They allow us to make reconstruction tests without acquisition problems.

5 Data segmentation

The purpose of this section is to addign a weight to each pixel of the image. The greater the weight the greater the contribution of this pixel to the reconstruction of the edge will be.

5.1 Pretreatments

Little pretreatment were done on the images under various modality. The speckle filtering or the use of enhancement contrast filter have a sure visual action but the reconstruction does not seem to be affected in our specific case. The only pretreatment used is an overlooked one. The ophthalmologist places four points on each image to isolate the lens and hence helps the treatment filters.

5.2 Treatments

To affect a weight to each pixel of the image, numerous edge detection filters were tested, using different methods, LOG, Canny-Deriche, Shen-Castan, and the operator based on the geometrical moments. The most convincing results were obtained with the Canny operator. It has been created as the solution of an optimization problem with constraints [3]. This filter is supposed to be an optimal compromise between the following criteria: localization, detection and unicity. We have to note that this filter is optimized for images flooded in a white, Gaussian, additive noise; and it is not the case in most of the used data.

This filter is actually one of the references in the edge detection for its quality of results; it is regularly used in the literature to the evaluation of new filters. A recursive implementation of this operator was developed by [4] allowing an important performance gain. The third dimension filter is obtained by supposing the filter separable and by making a convolution product. This choice is an easy one but it introduces anisotropies. These results images are difficult to use, and as recommended by [5], we extract its local maxima. This method consists in estimating the gradient direction and only keeping its watershed.

5.3 Post treatments

The previous stages can be applied to any type of images without taking into account their contents. Two post-treatments types are presented to take into account peculiarities of the eye contents. The first post-treatment consists to take into account ultrasound sound images and MRI particularities. The center of the eye have got no edges and generally the first visible edge is the good one. The "visible human" project images [10] have specifics characteristics. They are in fact photos of frozen tissues; crystals of ice are clearly visible in the vitrous, while it is uniform in the other modalities. A simple threshold is ineffective. The hysteresis threshold , introduced by [3] takes into account the edges connexity and luminance (levels of grey) and give us good results on such images.

6 Eyeball rebuilding with splines

The most used techniques for edge reconstruction on medical prints are snakes (active contour models) [7, 8]. A shape approaching the organ to be reconstructed is initialized, then deformed locally to fit the data. These deformations use, generally, physical properties of elasticity materials. These various methods allow the organ edge reconstruction of varied forms as bones, heart, brain, etc.. This type of reconstruction is effective but numerous parameters must be set. We opted for a different technique. The edge to be

reconstructed in our case is a quasi-spherical shape, and we reconstruct it by using B-splines. Their mathematical properties allow us to reconstruct the edge in a effective and fast way, and with adjusting only few parameters.

6.1 Principle

For a B-spline (1D) on $R = [a, b]$ we have to set:
— the degree k of the spline,
— the position and numbers of the knots $(\lambda_i, i = 0, ..., g+1)$,
— the coefficients c_i of the spline representation:

$$s(x) = \sum_{i=-k}^{g} c_i N_{i,k+1}(x),$$

where $N_{i,k+1}(x)$ is the B-spline basis function.

We have chosen to set the degree of the spline to 3. Tests indicate this is a good compromise between computer time and result quality. The other parameter determination depends on the approximation criteria used and the position of control knots.

6.1.1 *The Dierckx criteria [6]*

The Dierckx approximation criteria determine a spline like the solution of a constrained minimization problem:

minimize

$$\tilde{n} := \sum_{i=1}^{g} \left(s^{(k)}(\lambda_i +) - s^{(k)}(\lambda_i -) \right)^2$$

with the constraint

$$\delta := \sum_{r=1}^{m} (w_r(y_r - s(x_r)))^2 \leq S$$

where (x_r, y_r) are the coordinates of the m data points, with w_r the associated weight.

6.1.2 *Control knots number*

As the number of control knots becomes important, the smoothness of the curvature decreases. Using that property we set up an iterative algorithm to perform the calculation of the spline. After an initialization with few control knots (we set for example $\lambda_0 = a$, $\lambda_2 = b$ and $\lambda_1 = (a+b)/2$), the spline is computed. If the smoothness is too important (with the δ estimation) we add some control knots and we start again the estimation of the smoothness. In the other case we stop the algorithm. At each iteration we can insert one or more control knots. The distribution of the control knots is recomputed for each iteration. They can be linearly distributed over $R = [a, b]$.

This method can be generalized to surfaces without difficulty (see [6]) using spherical coordinates and periodic boundary conditions.

6.2 Results

Different results are presented either in 3d or 2d view. In 2d view, the spline is drawn in red, and represents the intersection of the 2d spline and the data volume. The main reconstruction errors are due to segmentation errors. But the more data the better, and the quality of the reconstruction needs to be good. The reconstruction of images issued from visible human (22 slices) is better than from the MRI (8 slices) and the ultrasound images (4 slices).

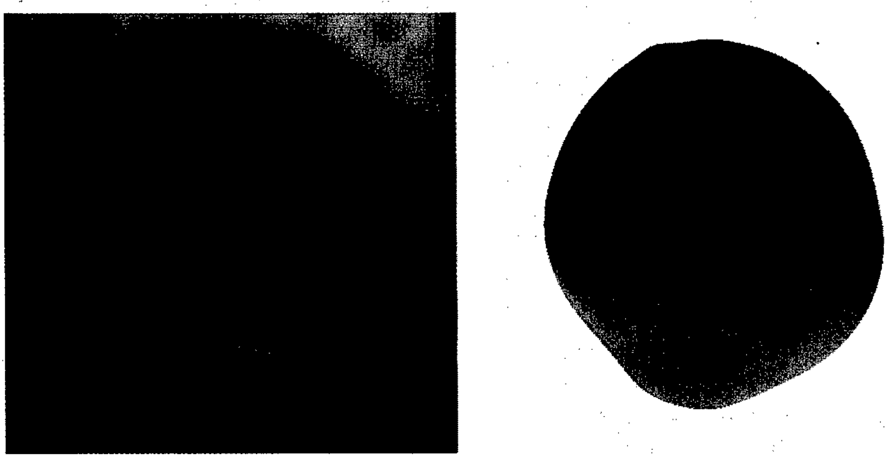

FIG. 1. Reconstruction using photographic images.

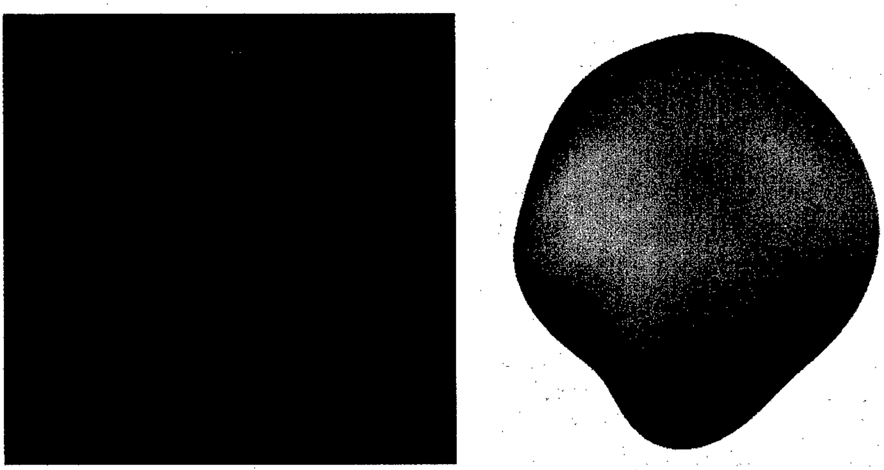

FIG. 2. Reconstruction using MRI.

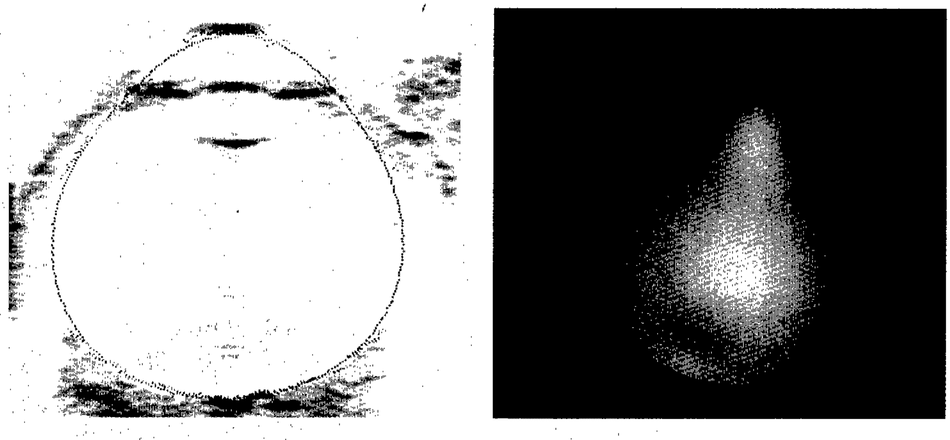

FIG. 3. Reconstruction using ultra sound images.

7 Elastic modelisation of surgery

7.1 Method used

The finite elements method is used to simulate surgery and solve the elasticity problem. Actually the knowledge of the comportment law of the eye ball tissues is the main limitation of this problem. Literature reports a wide range of coefficients to describe these tissues. In fact they seem to have an individual variability. So we use the approximation [9] for the elasticity coefficients which uses three parameters, internal pressure, radius of the eye and width of the edge. The use of complex models does not offer much information because of the low precision of the data that we used.

7.2 Results

Numerous simulations have been done. Results seem good in spite of the comportment law and the duration of the finite element method. The result are represented with a color map of the eye representing the curvature radius like the ophthalmologist does.

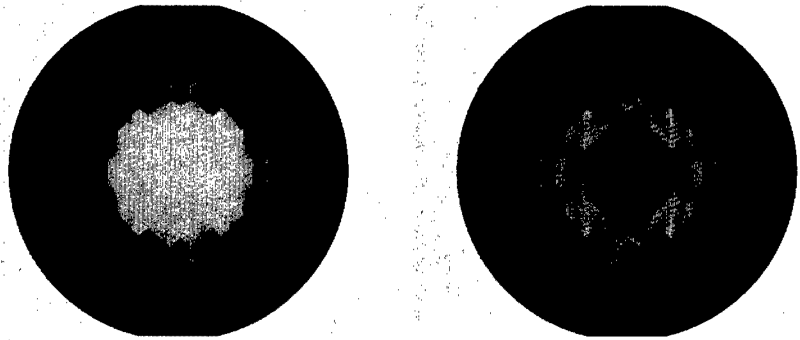

FIG. 4. Excimer Simulation before (left) and after (right).

8 Conclusion

This article presents a very modular path to realize modelisation of refractive surgeries. Each part of this work can be independently modified and can be adapted to an other organ. All this work has been validated by ophthalmologists. The eye ball reconstruction using spline appears to be an efficient method with a low CPU time. The mechanical modelisation provides proper results despite several approximations. This study might be useful for the medical doctor but also for testing new surgical techniques.

Bibliography

1. C. Dupas, La RMN au service de la medecine, *La Recherche* **81** (1977), 778–781.
2. S.D. Klyce, Computer assisted corneal topography : High resolution graphic presentation and analysis of keratoscopy, *Invest. Ophtalmol. Vi SCI.* **25** (1984), 1426–145.
3. J. Canny, A computational approach to edge detection. *IEEE Transaction on Pattern Analysis and Machine Intelligence.* **6** (1986), 679–698.
4. R. Deriche, Fast algorithms for low level vision, *IEEE Transaction on Pattern Analysis and Machine Intelligence.* **12** (1990), 78–87.
5. R. Deriche, Techniques d'extraction de contours, (http://www-sop.inria.fr/robotvis/personnel/der/der-eng.html) *Cours de l'INRIA Sophia-Antipolis*, 1998.
6. P. Dierckx, Curve and surface fitting with splines, Clarendon press, Oxford, 1995.
7. M. Klass A. Witkin D. Terzopulos, Snakes: active contour models, *Int J Comput Vision.* **1** (1988), 321–331.
8. D. Metaxas, Physics-based deformable models : Application to computer vision, graphics and medical imaging. (1996) Kluwer Academic.
9. P.P. Purslow W.S. Karwatowski, Ocular Elasticity, *Ophtalmology.* **103** (1996), 1686–1692.
10. http://www.nlm.nih.gov/research/visible/visible_human.html.